

Intermittent Fault Identification for Permanent Magnet AC Drives Based on the Short-Time Fourier Transform

Wesley G. Zanardelli, Elias G. Strangas, and Selin Aviyente
Department of Electrical and Computer Engineering
Michigan State University
East Lansing, MI 48824, USA
e-mail: zanardel@egr.msu.edu

Abstract—Prognosis for failure of an electric machine can be achieved through the detection of non-catastrophic faults. As the frequency of these types of faults increases, the working life of the machine is decreased, leading to eventual failure. In this work, two types of stator faults are studied. The methods developed are based on analysis of the Short-Time Fourier Transform of the field oriented machine currents. Linear discriminant analysis is used to classify between the fault types.

I. INTRODUCTION

Reliability of electrical machines and drives is an area of increased attention and research. Diagnosing correctly a failure in an electrical drive can lead to mitigation and continued operation, albeit at reduced power levels.

On the other hand, prior to the failure the drive can show signs of a developing fault, while it is operating normally. Detecting these early signs can lead to appropriate actions before a failure occurs. For the remainder of this paper the term fault is defined as a condition of the drive that allows for continued operation, but may eventually lead to failure.

Various methods to detect faults in electric machines were explored in [1]–[3]. In [1], Simulated faults were imposed on a 3-phase model of an interior permanent magnet motor under the assumptions of constant motor speed and constant current references. Switch-on and switch-off failures in the inverter were investigated. The authors showed the effect of the various faults on the Park’s vector pattern. In [2], a method to detect turn-turn insulation failures in induction machines was described. The line-neutral stator voltages were measured and filtered to remove the fundamental component of the machine excitation voltage. The RMS value of $v_{sum} = v_{an} + v_{bn} + v_{cn}$ of the filtered components is zero in a balanced machine, however in the case of turn-turn insulation failures, the number of shorted turns could be determined by the amplitude. In [3], BLDC machines were analyzed using parameter estimation in a model-based technique. Based on the inverter supply voltage, the DC current, and the mechanical speed, a least-squares method was used to estimate parameters in a model of the machine. The authors could determine whether the phase resistance of all coils had increased, indicating an increase in stator temperature, or a broken coil. Increases in Coulomb and viscose friction could also be detected.

Signal processing methods were used in [4] to analyze three-phase induction machines for the presence of broken rotor bars or end rings. An FFT is performed on the currents and a diagnostic index equal to the sum of the amplitude of the two sideband current components at $(1 \pm 2s)f$, where s is the slip of the machine, and f is the fundamental component of the current, is assigned. If the value of the diagnostic index exceeds a threshold, it is determined that either a broken rotor bar or end ring is present. Knowledge of the main nameplate data of the machine as well as the number of bars is required for this system.

The signal processing methods used in [5] were based on a Condition Monitoring Vector Database to find the presence of broken rotor bars in induction machines. First a set of Condition Monitoring Vectors (*CMV*) were determined through simulations using the time-stepping Finite Element (TSFE) technique, and a single vector was computed for each complete AC cycle, both in the presence and absence of a fault. The *CMV* is defined in (1),

$$CMV = \begin{bmatrix} \frac{V_n}{V_p} & \frac{I_n}{I_p} & \frac{Z_n}{Z_p} & A(f_{LSB}) & \Delta\delta_{BB} & \Delta\delta_{SC} & \omega_m & T_{dev} \end{bmatrix} \quad (1)$$

where V , I , and Z with the subscripts n and p are the negative and positive sequence components of the stator voltages, currents, and associated impedances; $A(f_{LSB})$ is the amplitude of the low sideband frequency spectrum component of the stator current at the frequency $(1 - 2s)f_s$, where f_s is the power supply frequency; $\Delta\delta_{BB}$ and $\Delta\delta_{SC}$ represent the range of oscillation of the resultant mid air-gap magnet field for broken rotor bars and stator winding inter-turn faults; and ω_m and T_{dev} are the motor speed and developed motor torque respectively.

Finally, an artificial, intelligence-based statistical machine learning approach, using Gaussian Mixture Models, was used to train a Bayesian maximum likelihood classifier. Experimental results showed that the algorithm could discern between various numbers of broken rotor bars.

In our previous work, a wavelet based failure prognosis method was developed for brush DC motors [6]. The modulus maxima of the Discrete Wavelet Transform (DWT) of the DC current was analyzed. An algorithm to detect the presence of a fault was based on thresholding of the analysis coefficients. If

the detection criterion was met, the coefficients were passed to a classification algorithm. Three classification algorithms were evaluated. The first was based on a decision tree, the second was based on the nearest neighbor rule, and the third was based on linear discriminant analysis. Classification was possible between DC currents in machines with the following faults: increased coil resistance, increased friction, faulty brush springs, rotor misalignment, and damaged commutator face.

Next, a failure prognosis method based on wavelet analysis was developed for PMAC drives [7]. Two electrical faults were investigated there. The first was a momentary increased resistance in one phase due to a bad connection between the motor and the controller and the second was a turn-to-phase short in the stator windings. Analysis was performed on the Undecimated Discrete Wavelet Transform (UDWT) of the torque producing component of the field oriented stator currents. First, a detection algorithm was based on thresholding of the energy in the wavelet coefficients. If the detection criterion was met, the coefficients were passed to a classification algorithm based on linear discriminant analysis to discriminate between the two faults.

In the present work, a failure prognosis system is developed to detect signs of developing stator faults in PMAC drives. Compared to previous work, the methods developed are based on the Short-Time Fourier Transform (STFT). Although wavelets have many advantages over Fourier methods for analysis of nonstationary signals, there are some advantages to using the STFT. The resultant STFT coefficients are more intuitive and easier to correlate with physical phenomena. Unlike the DWT, where each successive scale has half the coefficients of the previous, the STFT has the same number of coefficients at each time instant. The frequency axis for the STFT is linear, compared to the logarithmic scale axis in the wavelet transform. Also, compared to the UDWT, the STFT produces fewer coefficients, thus requiring less storage space for the classification algorithm.

Two types of stator faults are explored, both electrical. The first fault is a momentary increased resistance in one phase due to a bad connection between the motor and the controller. The second fault is a turn-to-phase short, simulating an insulation failure in the stator windings of the motor.

The algorithm is based on analysis of the STFT of the torque producing component of the field oriented stator currents. Thresholding on the energy in the STFT is used to detect a fault in the machine, and linear discriminant analysis is used to classify between the fault types. A collection of observed data is used to train the detection and classification components of the algorithm.

The algorithms developed can be implemented in an online system, using extra processing time in the motor controller.

II. THEORETICAL BASIS

A. Short-Time Fourier Transform

The Fourier Transform gives the spectrum of a signal. It is best suited for the analysis of stationary signals, or signals whose spectrum remains constant. The FFT is used

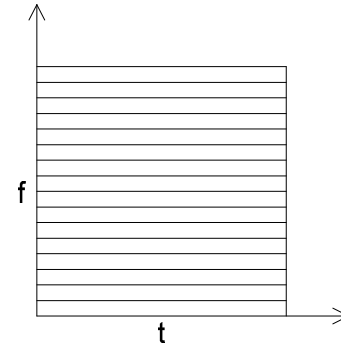


Fig. 1. FFT Tiling

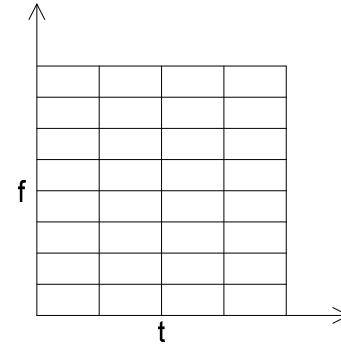


Fig. 2. STFT Tiling

to determine the spectrum of discrete-time signals. Tiling in the time-frequency plane for the FFT in Fig. 1 shows that the spectrum of the signal is divided into several frequency bands, however no information is present on the time axis. The faults studied in this work manifest themselves as short transients superimposed on the stator currents. Analysis of these short transients, however, requires information in both frequency and time. The inability to provide time localization of a signal is a fundamental limitation of the FFT.

The STFT [8] is an extension of the FFT, allowing for the analysis of non-stationary signals. Here, the signal is broken up into small time sections, and each is analyzed using the FFT. The results for of the STFT are intuitive and easy to correlate with the original signal. Tiling for the STFT in Fig. 2 shows how the spectrum of a signal changes with time. The tiling for the STFT is uniform in both time and frequency. In the implementation of the STFT, a design tradeoff must be made between time and frequency resolution. This is due to the uncertainty principle, which limits the lower bound on the time-bandwidth product (2).

$$TB \geq \frac{1}{2} \quad (2)$$

A block diagram for the STFT algorithm is shown in Fig. 3, where $nfft$ is the length of the DFT, $overlap$ is the number of samples the two frames overlap, and $window$ is a weighting vector applied to the FFT input. The spectrogram is a plot of the magnitude square of the STFT. It is similar to the tiling

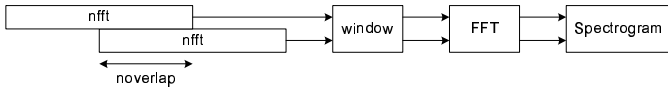


Fig. 3. STFT Block Diagram

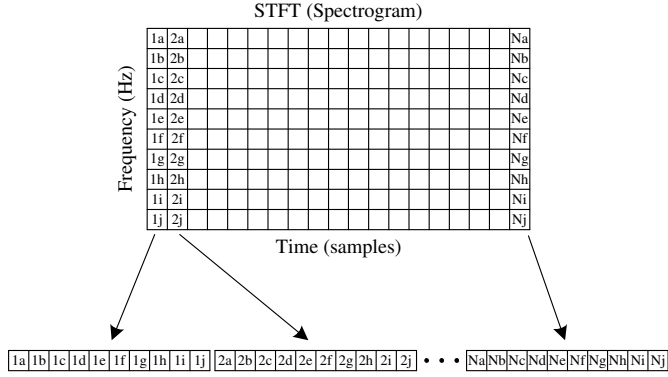


Fig. 4. Vectorization of N Samples of the STFT

shown in Fig. 2, with color shading denoting the energy in each tile.

B. Pattern Recognition

Once the STFT coefficients have been determined, the presence of a fault is detected based on thresholding of the energy in the coefficients. The next step is to vectorize the coefficients allowing for the use of discriminant analysis for classification. The vectorization process combines columns of the STFT into a vector. Vectorization of the data begins when the criterion for detection is met. An example of vectorization using N time samples is shown in Fig. 4.

In the implementation of discriminant functions, no prior knowledge of a probability distribution among the sample points is assumed. The space is divided into K regions, each having its own weighting coefficients. In this work, we use linear discriminant functions (3) [9],

$$D_k(\mathbf{x}) = x_1\alpha_{1k} + x_2\alpha_{2k} + \dots + x_N\alpha_{Nk} + \alpha_{N+1,k} \quad (3)$$

$$k = 1, 2, \dots, K$$

where x is the N -dimensional sample vector and α are the normalized weighting coefficients for the k -th class. A sample vector belongs to a particular class if its discriminant function is greater for that class than for any other class, i.e., \mathbf{x}_i belongs to class C_j if

$$D_j(\mathbf{x}) > D_k(\mathbf{x}) \quad \text{for every } k \neq j.$$

The weighting coefficients are adjusted from their initial guess through a training procedure using sample vectors which the proper classification is known. The algorithm for this procedure makes adjustments to the weighting coefficients until each sample vector is correctly classified.

Young and Calvert [9] show that this training algorithm will converge in a finite number of steps. When a sample vector is

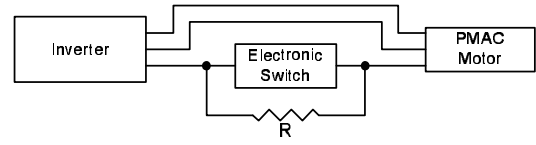


Fig. 5. Experimental Mimic of Series Resistance Fault

correctly classified, no adjustment to the weighting coefficients is made. When a sample vectors is incorrectly classified, or

$$D_j(\mathbf{x}) \leq D_l(\mathbf{x}),$$

where

$$D_l(\mathbf{x}) = \max_{l \neq j} [D_1(\mathbf{x}), \dots, D_K(\mathbf{x})],$$

adjustments are made to α_j (4) and α_l (5) only,

$$\alpha_j(i+1) = \alpha_j(i) + a\mathbf{x}_i \quad (4)$$

$$\alpha_l(i+1) = \alpha_l(i) - a\mathbf{x}_i, \quad (5)$$

where a is a gain constant.

Discriminant functions have minimal storage requirements after the training phase since, for each class, only a single vector of weighting coefficients need to be stored. Storage of training samples is no longer required during the classification phase. For multiclass problems ($K > 2$), it can be said that the classes are linearly separable if linear discriminant functions $D_1(\mathbf{x}), \dots, D_K(\mathbf{x})$ exist, such that (6) is true.

$$D_j(\mathbf{x}) > D_k(\mathbf{x}) \quad \text{for every } \mathbf{x} \text{ in } C_j \text{ and all } k \neq j \quad (6)$$

III. FAULTS EXPLORED

The test machine used in this analysis is a six-pole surface mounted PMAC machine for an automotive application. The machine is operated in a vector drive with the torque angle set to $\pi/2$ [10]. This mode of operation minimizes losses in the machine, and is suitable for operating speeds up to the base speed. The torque-producing component of the stator current command was $i_{qs}^* = 0.3pu$, and the flux-weakening component $i_{ds}^* = 0$; the speed is controlled by the dynamometer and is set to 1/10 the no-load speed.

The faults imposed in this work are not periodic. The time interval between successive faults is random, as well as the fault duration.

A. Series Resistance

The first fault explored in this work is an intermittently increased contact resistance between the motor and the controller. An experiment was designed to simulate this. The fault is achieved by adding the parallel combination of a normally closed switch, and a resistance in series with one of the motor phases as shown in Fig. 5.

The fault is initiated by opening the switch for a short time interval, causing current to flow through the resistance. The switch is described in detail in Section V.

The value of the series resistance is approximately ten times the value of the stator resistance, R_s . The fault is

initiated as the phase current command rises to 95% of its peak amplitude. Tests with fault durations of $5ms$ and $10ms$ have been performed to investigate invariance of the results with respect to this parameter.

B. Turn-To-Phase Short

The second fault explored in this work is an insulation failure in the stator windings of the motor. The machine used in this experiment has multiple parallel stranded-wire windings per phase, each with several coils in series. To simulate this fault in the experimental setup, at one point in a single strand of one of the windings, the insulation was removed, and a normally open switch was added between this point and the corresponding phase terminal of the motor. The fault was initiated by momentarily closing the switch, causing current to be split between the intended path and the switch.

The fault is initiated as the phase current command rises to 95% of its peak amplitude. Tests with fault durations of $5ms$ and $10ms$ have been performed to investigate invariance of the results with respect to this parameter.

IV. FAULT DETECTION AND CLASSIFICATION

The detection and classification of the faults described in Section III are based on analysis of the stator currents of the machine. Rather than analyzing the three phase stator currents independently of each other, the field oriented currents i_{qs} and i_{ds} are used. This has the advantage that the fundamental electrical frequency is not present. Additionally, these signals are already present in the controller and require no additional hardware or computation. Consequently, rotor speed has little effect on the spectrum of these currents, allowing for invariance in the algorithm to rotor speed. Together, i_{qs} and i_{ds} are a complete representation of the stator currents, however, it has been determined experimentally that through analysis of i_{qs} only, accurate fault detection and classification can be achieved.

The controller time constant is longer than the transients that occur at the edges of the faults explored in this work. While the selection of gains in the controller has a significant effect on the currents during and after a fault occurs, controller correction of the currents has a negligible effect on the transients at the inception and the clearing of a fault.

The input to the detection and classification algorithm is a subset of the STFT of the measured q-axis current, i_{qs} . For this analysis, vectorization of 5 time samples, or $4ms$, of data occurs. This time interval is used to capture the beginning and end of each fault separately.

The algorithm has two parts; a detection phase and a classification phase. The detection phase of the algorithm is based on thresholding on the time marginal of the STFT. The time marginal is defined as the energy at each time instant in the STFT. The threshold on the time marginal was set to be 25% greater than the largest which was observed in all samples from the healthy machine data. If the time marginal in new test data exceeds this threshold, a fault is considered to exist.

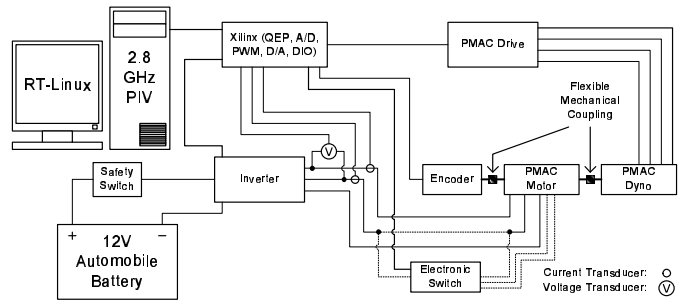


Fig. 6. Experimental Setup Block Diagram

The classification phase was based on linear discriminant analysis. This phase is implemented when the criterion for detection is met. Since the fault duration is random, two distinct events were assigned to each intermittent fault; one corresponding to the inception, and the other to the clearing of the fault. The advantage of two separate classes for each fault is invariance to the duration of the fault. Additionally, a postprocessing algorithm to verify that subsequent classification of the beginning and end of the same fault type would further confirm existence of the fault. To train the algorithm, thereby determining the weighting coefficients, data were used from 16 experiments corresponding to both faults with $5ms$ and $10ms$ switch durations. The data used were the 5 samples in the STFT corresponding to each event.

Following the training of the weighting coefficients, data that had not been used in the training algorithm were tested. Two data sets from each of the following operating conditions were tested: Healthy, $5ms$ series resistance, $10ms$ series resistance, $5ms$ turn-to-phase short, and $10ms$ turn-to-phase short.

FEA results using a commercial package, Flux2D, were considered for use in training the detection and classification algorithms, however the spectrum of the preliminary FEA results was significantly different than that of the experimental results. The use of FEA would allow for increased flexibility, giving more training samples, for the faults explored. Fault detection approaches based on results from FEA were introduced in [5], however the faults of interest were limited to low-frequency phenomena (i.e. broken rotor bars), compared to the faults studied in this work.

V. EXPERIMENTAL SETUP

A block diagram for the experimental setup is shown in Fig. 6. A PC running RT-Linux was used as the controller for this project. The PC is superior to a DSP in terms of cost, CPU power, and memory capacity. A fundamental limitation of the PC, however, is the limited I/O capability. To remedy this, a custom Xilinx FPGA based I/O board was developed. The I/O board inputs include 12 analog channels and a counter for a quadrature encoder. Outputs include 12 PWM/digital and 4 analog channels. Communication between the I/O board and the PC is via the parallel port.

Two phase currents were measured using current transducers

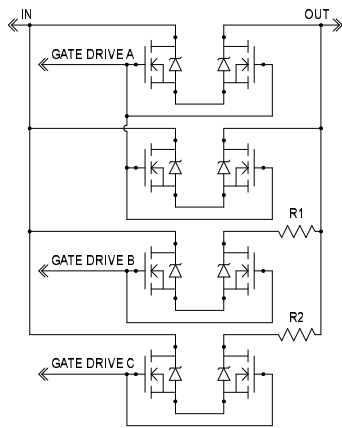


Fig. 7. Electronic Switch

with rated accuracy of 0.45% and bandwidth of 0–200kHz. A single line-line voltage for use in the initial position calibration was measured as well.

A quadrature encoder with 1024 counts per revolution (4096 for quadrature) and an index pulse was used to measure the rotor position.

A bi-directionally conducting electronic switch was designed to initiate faults in the stator. This switch, as shown by the dotted lines in Fig. 6, can be configured to initiate either the series resistance fault or the turn-to-phase short. A circuit diagram for the electronic switch is shown in Fig. 7. $R_{DS(ON)}$ for each MOSFET is approximately one-third the resistance of a single turn of a single strand in one of the stator coils. The switch can be controlled using digital outputs or PWM to create a resistance profile.

VI. RESULTS

The results from two typical test cases are shown in Fig. 8.

On the left side of Fig. 8 are results from the series resistance fault, and on the right side are results from the turn-to-phase short. The first row shows the q-axis, or torque producing component, of the current. The second row shows the STFT of the above currents. The third row shows the output of the detection and classification algorithm, with 0=healthy, 1=beginning of series resistance fault, 2=end of series resistance fault, 3=beginning of turn-to-phase short, and 4=end of turn-to-phase short. The results presented are based on new data not used in the training set.

In Fig. 8, it can be seen that the magnitude of the STFT coefficients is increased at the points of inception and clearing of the faults. The increased energy at these points meets the criterion for detection, and the classification algorithm operates on the STFT coefficients corresponding to 4ms of data at these points. The results shown indicate correct classification of the inception and clearing of both faults explored in this work.

The ten tests described in Section IV resulted in no false positives. In the two healthy cases, no fault events were detected. In the four cases with the series resistance fault, all fault inception and clearing events were identified correctly. In

the four cases with the turn-to-phase short, all fault inception and clearing events were identified correctly.

VII. CONCLUSIONS

An algorithm capable of giving a prognosis for failure of a PMAC drive has been developed. It is based on the detection and classification of small transients in the stator current corresponding to non-catastrophic faults.

Unlike prior methods, the method proposed here is capable of recognizing steady fault conditions as well as the transient phenomena associated with intermittent faults which can develop into a catastrophic fault, and evaluating their severity and frequency. Early detection of these faults can give indication when maintenance or mitigation is required, minimizing the likelihood of system failure. This work addresses the limitation of existing methods which can only detect permanent faults in drives.

The categorization algorithm uses a linear discriminant function and is trained using a set of operating conditions which include healthy drives and samples of faulted drives. An exhaustive set of such conditions is necessary to develop a robust algorithm.

Although the algorithms in this work were used offline, they can be added to an existing motor controller enabling them to run close to real-time. The vector currents are typically calculated as part of the control. Minimal, if any, additional CPU speed and memory capacity would be required ensuring a low-cost system. The training phase of the algorithms would remain offline.

ACKNOWLEDGMENT

The authors thank Drs. Tomy Sebastian, Sayeed Mir, Mohammad Islam, and Avoki Omekanda from Delphi Corporation for their continued guidance and support in this research project.

REFERENCES

- [1] N. Bianchi, S. Bolognani, and M. Zigliotto, "Analysis of PM synchronous motor drive failures during flux weakening operation," in *27th Annual IEEE Power Electronics Specialists Conference*, vol. 2, Jun 1996, pp. 1542–1548.
- [2] A. Cash, T. G. Habetler, and G. B. Kliman, "Insulation failure prediction in AC machines using line-neutral voltages," *IEEE Transactions on Industry Applications*, vol. 34, pp. 1234–1239, Nov.–Dec. 1998.
- [3] O. Moseler and R. Isermann, "Application of model-based fault detection to a brushless DC motor," *IEEE Transactions on Industrial Electronics*, vol. 47, pp. 1015–1020, Oct 2000.
- [4] A. Bellini, F. Filippetti, G. Franceschini, C. Tassoni, R. Passaglia, M. Saottini, G. Tontini, M. Giovannini, and A. Rossi, "On-field experience with online diagnosis of large induction motors cage failures using MSCA," *IEEE Transactions on Industry Applications*, vol. 38, pp. 1045–1053, Jul–Aug 2002.
- [5] C. C. Yeh, B. Mirafzal, R. J. Povinelli, and N. A. O. Demerdash, "A condition monitoring vector database approach for broken bar fault diagnostics of induction machines," in *International Electric Machines and Drives Conference*, May 2005, pp. 29–34.
- [6] W. G. Zanardelli, E. G. Strangas, H. K. Khalil, and J. M. Miller, "Wavelet-based methods for the prognosis of mechanical and electrical failures in electric motors," *Mechanical Systems and Signal Processing*, pp. 411–426, Mar. 2005.
- [7] W. G. Zanardelli, E. G. Strangas, and S. Aviyente, "Failure prognosis for permanent magnet AC drives based on wavelet analysis," in *International Electric Machines and Drives Conference*, May 2005, pp. 64–70.

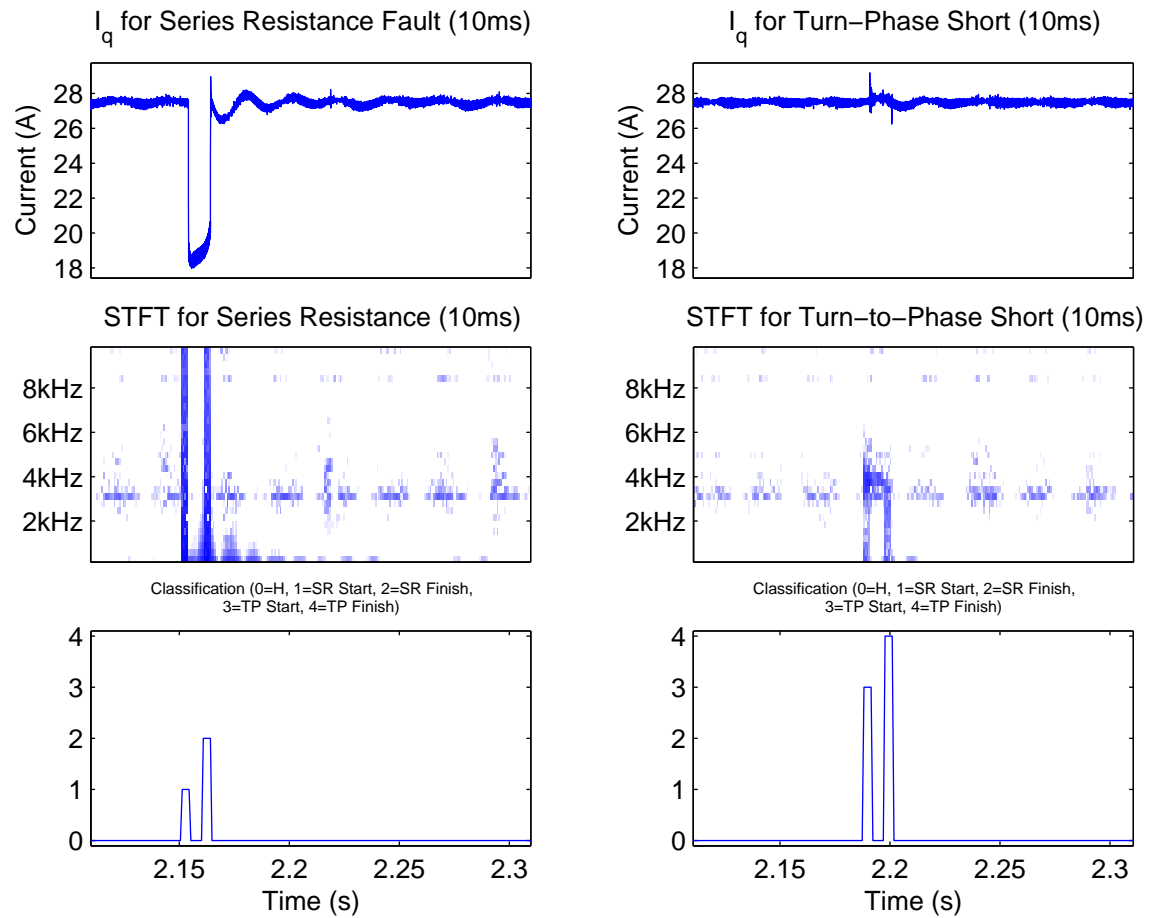


Fig. 8. Typical Results

- [8] L. Cohen, *Time-Frequency Analysis*. Prentice Hall, 1995.
- [9] T. Y. Young and T. W. Calvert, *Classification, Estimation and Pattern Recognition*. American Elsevier Publishing Co., Inc., 1974.
- [10] R. Krishnan, *Electric Motor Drives: Modeling, Analysis, and Control*. Prentice Hall, 2001.